

available at [www.sciencedirect.com](http://www.sciencedirect.com)journal homepage: [www.elsevier.com/locate/chnjc](http://www.elsevier.com/locate/chnjc)

## Article

# Fructose-catalyzed synthesis of tetrahydrobenzo[*b*]pyran derivatives: Investigation of kinetics and mechanism



Sayyedah Shadfar Pourpanah, Sayyed Mostafa Habibi-Khorassani\*, Mehdi Shahraki

Department of Chemistry, University of Sistan and Baluchestan, Zahedan, Iran

## ARTICLE INFO

## Article history:

Received 16 December 2014

Accepted 19 January 2015

Published 20 May 2015

## Keywords:

Fructose

Catalyst

Kinetics

Mechanism

Tetrahydrobenzo[*b*]pyran derivative

## ABSTRACT

Fructose was used as an efficient catalyst for three-component condensation reactions of aryl aldehydes, malononitrile, and dimedone in a mixture of EtOH and H<sub>2</sub>O as green solvents. The advantages of this method are a short reaction time, high yields, low cost, easy accesses, and simple work-up. The mechanism of the synthesis of a derivative of 4*H*-tetrahydrobenzo[*b*]pyran was clarified using spectroscopic kinetic methods. The activation energy ( $E_a = 65.34$  kJ/mol) and related kinetic parameters ( $\Delta G^\ddagger = 69.14$  kJ/mol,  $\Delta S^\ddagger = 20.99$  J/(mol·K), and  $\Delta H^\ddagger = 62.89$  kJ/mol) were calculated, based on the effects of temperature, concentration, and solvent. The first step in the proposed mechanism was identified as the rate-determining step ( $k_1$ ), based on the steady-state approximation.

© 2015, Dalian Institute of Chemical Physics, Chinese Academy of Sciences.

Published by Elsevier B.V. All rights reserved.

## 1. Introduction

Tetrahydrobenzo[*b*]pyran derivatives are important in drug research because of their various biological and pharmacological activities such as spasmolytic, diuretic, anticoagulant, anticancer, antianaphylactic, antioxidant, antileishmanial, antibacterial, antifungal, hypotensive, antiviral, antiallergenic, and antitumor activities [1–6]. They can also be used as cognitive enhancers for the treatment of neurodegenerative diseases, including Alzheimer's disease, amyotrophic lateral sclerosis, Huntington's disease, Parkinson's disease, AIDS-associated dementia, and Down's syndrome, and for the treatment of schizophrenia and myoclonus [7]. Some 4*H*-benzo[*b*]pyran derivatives are useful as photoactive materials [8]. Consequently, many methods for the synthesis of these compounds have been reported, including the use of microwave [9] and ultrasonic irradiations [10], sodium bromide [10], hexadecyl-dimethylbenzylammonium bromide [11], tetramethylammo-

nium hydroxide [12], diammonium hydrogen phosphate [13], fluoride ions [14], magnesium oxide [15], sodium selenite [16], iodine [17], H<sub>6</sub>P<sub>2</sub>W<sub>12</sub>O<sub>62</sub>·H<sub>2</sub>O [18], tetrabutylammonium bromide [19], cerium(III) chloride [20], lithium bromide [21], RE(PFO)<sub>3</sub> (RE: rare earth) [22], Amberlite IRA-40 (OH) [23], acidic ionic liquids [24], L-proline [25], ZnO-β-zeolite [26], trisodium citrate [27], and basic ionic liquids [28]. Most of these synthetic methods suffer from drawbacks such as the use of toxic catalysts, strong basic conditions, expensive and complex catalysts or reagents, many tedious steps, and, in most cases, low product yields and long reaction time; these restrict use of these derivatives in practical application.

Recently, organic reactions in green solvents such as H<sub>2</sub>O, EtOH, and H<sub>2</sub>O-EtOH mixture have attracted much attention, because they are cheap, safe, and environmentally benign [29,30]. They also avoid the use of harmful organic solvents. In a continuation of our research on using cheap, easily accessible, biodegradable, green catalysts and solvents [31–34], we de-

\* Corresponding author. Tel/Fax: +98-541-2446565; E-mail: [smhabibi@chem.usb.ac.ir](mailto:smhabibi@chem.usb.ac.ir)

This work was supported by the Research Council of the University of Sistan and Baluchestan.

DOI: 10.1016/S1872-2067(14)60302-8 | <http://www.sciencedirect.com/science/journal/18722067> | Chin. J. Catal., Vol. 36, No. 5, May 2015

veloped new synthetic methods for the preparation of tetrahydrobenzo[*b*]pyran derivatives using aryl aldehydes (**1**), malononitrile (**2**), and dimedone (**3**) in the presence of fructose as a catalyst in H<sub>2</sub>O-EtOH at 40 °C (Fig. 1). This is a one-pot, three-component reaction in EtOH-H<sub>2</sub>O; it is operationally simple, clean, and efficient, and consistently gives the corresponding products in good to excellent yields. In recent years, we have tried to expand experimental and theoretical studies on the kinetics and mechanisms of some organic reactions [35–38]. In this study, we used ultraviolet-visible (UV-Vis) and dynamic <sup>1</sup>H nuclear magnetic resonance (NMR) spectroscopies, and theoretical calculations to elucidate the detailed kinetics and mechanisms of these reactions. We report, for the first time, kinetic results together with detailed mechanistic studies of the synthesis of a derivative of 4*H*-tetrahydrobenzo[*b*]pyran, based on a global kinetic analysis method using UV-Vis spectroscopy.

## 2. Experimental

### 2.1. Chemicals and equipment

All reagents were purchased from Merck and Aldrich, and used without purification. All yields refer to isolated products after purification. The products were identified by comparison of their physical data with those of authentic samples, and from infrared (IR) and NMR spectroscopic data. NMR spectra were recorded using a Bruker Avance DRX 400 MHz instrument. The spectra were measured in DMSO-*d*<sub>6</sub> relative to tetramethylsilane (0.00 ppm). IR spectra were recorded using a JASCO FT-IR 460Plus spectrophotometer. Melting points were determined in open capillaries, using an electrothermal 9100 melting-point apparatus. Thin-layer chromatography (TLC) was performed on silica-gel Polygram SILG/UV 254 plates. Rate constants are presented as averages of several kinetic runs (at least 6–10) and are reproducible within ±3%. The overall reaction was determined by monitoring the absorbance changes of the products with time, using a Varian (Model Cary Bio-300) UV-Vis spectrophotometer with a 10 mm light-path cell. The reaction temperature was maintained to within ±0.1 °C at various temperatures, using a circulating water bath.

### 2.2. General procedure for synthesis of tetrahydrobenzo[*b*]pyran derivatives

Fructose (20 mol%) was dissolved in H<sub>2</sub>O-EtOH (2:1) and an aryl aldehyde (1 mmol), malononitrile (1 mmol), and dimedone (1 mmol) were added to the solution at 40 °C. The progress of the reaction was monitored by TLC. When the reaction was

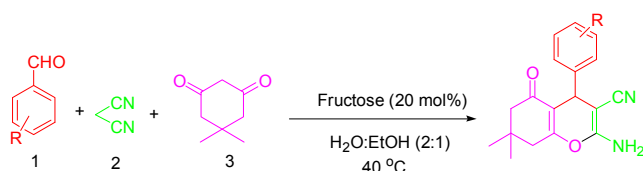


Fig. 1. Synthesis of tetrahydrobenzo[*b*]pyran derivatives in presence of fructose.

complete, the mixture was cooled to room temperature and the products were isolated by filtration, washed with H<sub>2</sub>O, and recrystallized from EtOH (95%) to afford pure products.

Selected spectroscopic data of some products are given below.

2-Amino-5,6,7,8-tetrahydro-7,7-dimethyl-5-oxo-4-phenyl-4*H*-chromene-3-carbonitrile (Table 3, entry 1). IR (KBr, cm<sup>-1</sup>): 3390, 3245, 2960, 2190, 1676, 1209; <sup>1</sup>H NMR (400 MHz, CDCl<sub>3</sub>): δ (ppm) = 1.07 (s, 3H), 1.14 (s, 3H), 2.25 (dd, *J* = 16.4 Hz, 2H), 2.48, (s, 2H), 4.43 (s, 1H), 4.55 (s, 2H), 7.2, 7.3 (m, 5H).

2-Amino-5,6,7,8-tetrahydro-4-(2,3-dimethoxyphenyl)-7,7-dimethyl-5-oxo-4*H*-chromene-3-carbonitrile (Table 3, entry 7). IR (KBr, cm<sup>-1</sup>): 3305, 3205, 2945, 2175, 1676, 1212; <sup>1</sup>H NMR (400 MHz, DMSO-*d*<sub>6</sub>): δ (ppm) = 1.08 (s, 3H), 1.12 (s, 3H), 2.22 (dd, *J* = 16 Hz, 2H), 2.44 (dd, *J* = 17.6, 2H), 3.85 (s, 3H), 3.95 (s, 3H), 4.52 (s, 2H), 4.74 (s, 1H), 6.716–6.809 (dd, *J* = 8, 2H), 6.972 (t, *J* = 8, 1H).

2-Amino-5,6,7,8-tetrahydro-4-(4-methyl)-7,7-dimethyl-5-oxo-4*H*-chromene-3-carbonitrile (Table 3, entry 11). IR (KBr, cm<sup>-1</sup>): 3465, 3320, 2955, 2190, 1676, 1247; <sup>1</sup>H NMR (400 MHz, DMSO-*d*<sub>6</sub>): δ (ppm) = 1.08 (s, 3H), 1.12 (s, 3H), 2.23 (dd, *J* = 16.4 Hz, 2H), 2.30 (s, 3H), 2.40 (dd, *J* = 17.6, 2H), 4.52 (s, 2H), 4.74(s, 1H), 6.716–6.809 (m, 2H), 6.972 (t, 1H).

## 3. Results and discussion

### 3.1. Optimization of synthetic conditions

We studied the reaction of benzaldehyde (1 mmol), malononitrile (1 mmol), and dimedone (1 mmol) to optimize the reaction conditions. As the data in Tables 1 and 2 show, the best results were obtained at 40 °C in the presence of 0.036 g (20 mol%) fructose in H<sub>2</sub>O-EtOH (2:1).

The scope and efficiency of the reaction under the optimum conditions were explored for the synthesis of a wide variety of substituted tetrahydrobenzo[*b*]pyran derivatives from aryl aldehydes, malononitrile, and dimedone. The results are summarized in Table 3.

Table 1

Effects of various solvents on synthesis of tetrahydrobenzo[*b*]pyran derivatives in presence of fructose (20 mol%) at 40 °C.

Entry	Solvent	Time (min)	Yield (%)
1	EtOH	150	44
2	H <sub>2</sub> O	160	51
3	H <sub>2</sub> O-EtOH (3:1)	70	50
4	H <sub>2</sub> O-EtOH(2:1)	45	86
5	H <sub>2</sub> O-EtOH(1:1)	50	68
6	H <sub>2</sub> O-EtOH(2:1)	60	40

Table 2

Effect of amount of catalyst on synthesis of tetrahydrobenzo[*b*]pyran derivatives at 40 °C.

Entry	Catalyst (mol%)	Yield (%)
1	5	58
2	10	73
3	15	70
4	20	86
5	25	75
6	30	73

**Table 3**

Synthesis of tetrahydrobenzo[*b*]pyran derivatives via condensation of aryl aldehydes (**1**), malononitrile (**2**), and dimedone (**3**) in the presence of fructose (20 mol%) in H<sub>2</sub>O-EtOH (2:1) at 40 °C.

Entry	Aromatic aldehyde	Time (min)	Yield (%)	Melting point (°C)	
				Observed	Reported
1	C <sub>6</sub> H <sub>5</sub> CHO	45	86	227–228	226–228 [15]
2	4-ClC <sub>6</sub> H <sub>4</sub> CHO	80	78	208–209	207–209 [26]
3	2-ClC <sub>6</sub> H <sub>4</sub> CHO	85	72	206–208	208–210 [39]
4	2,4-(Cl) <sub>2</sub> C <sub>6</sub> H <sub>3</sub> CHO	75	67	118–120	115–117 [22]
5	4-(OMe)C <sub>6</sub> H <sub>4</sub> CHO	60	36	193–195	196–198 [26]
6	Thiophene-2-carbaldehyde	165	76	218–220	210–212 [14]
7	2,3-(OMe) <sub>2</sub> C <sub>6</sub> H <sub>3</sub> CHO	60	71	217–219	216–218 [40]
8	2-NO <sub>2</sub> C <sub>6</sub> H <sub>5</sub> CHO	15	87	217–219	220–222 [39]
9	3-NO <sub>2</sub> C <sub>6</sub> H <sub>5</sub> CHO	10	85	208–210	212–214 [15]
10	4-NO <sub>2</sub> C <sub>6</sub> H <sub>5</sub> CHO	10	89	176–178	177–178 [26]
11	4-MeC <sub>6</sub> H <sub>5</sub> CHO	10	89	208–211	214–216 [12]
12	2-Furaldehyde	135	60	218–220	222–224 [12]

Various aryl aldehydes with electron-withdrawing or electron-releasing substituents (*ortho*-, *meta*-, and *para*-substituted) participated well in this reaction and gave the products in good to excellent yields.

We propose the following mechanism for the synthesis of a tetrahydrobenzo[*b*]pyran derivative in the presence of fructose as a catalyst. First, Knoevenagel condensation between 4-nitrobenzaldehyde (**1**) and malononitrile (**2**) produces 2-benzylidenemalononitrile (**I<sub>1</sub>**). Michael addition of **I<sub>1</sub>** with dimedone (**3**), followed by cyclization and tautomerization, affords the corresponding product **4** (Fig. 2).

### 3.2. Kinetics

To gain an insight into the mechanism of tetrahydrobenzo[*b*]pyran derivative synthesis, a kinetic study of the reaction of 4-nitrobenzaldehyde (**1**), malononitrile (**2**), and dimedone (**3**) in the presence of fructose in H<sub>2</sub>O-EtOH (2:1) was performed using UV-Vis spectroscopy. First, it was necessary to find an appropriate wavelength for the kinetic study. A solution (10 mmol/L) of each reactant, i.e., **1**, **2**, and **3**, and a fructose solution (25 mmol/L) were prepared in H<sub>2</sub>O-EtOH (2:1). An aliquot (approximately 3 mL) of each reactant was pipetted into a 10 mL light-path quartz spectrophotometer cell, and the spectrum of each compound was recorded at 25 °C over the wavelength range 200–600 nm. In the second experiment, aliquots (0.2 mL) of a solution (40 mmol/L) of fructose and of reactants **1** and **3** were pipetted into a quartz spectrophotometer cell and then an aliquot (0.8 mL) of a solution (4 mmol/L) of reactant **2** was added to the mixture, according to the stoichiometry of each reactant in the overall reaction. The reaction was monitored by recording scans of the entire spectra at 20 min intervals during the reaction, at ambient temperature (Fig. 3). As Fig. 3 shows, the appropriate wavelength was 385 nm (corresponding mainly to product **4**). At this wavelength, reactants **1**, **2**, **3**, and fructose have almost no absorbance, which provides practical conditions for kinetic and mechanistic investigations of the reaction. In all the experiments, the UV-vis spectrum of the product was measured over the product concentration range from 0.1 to 10 mmol/L to confirm the linear

relationship between the absorbance and concentrations values.

The reaction kinetics was followed based on the UV absorbance measurements with respect to time at the same con-

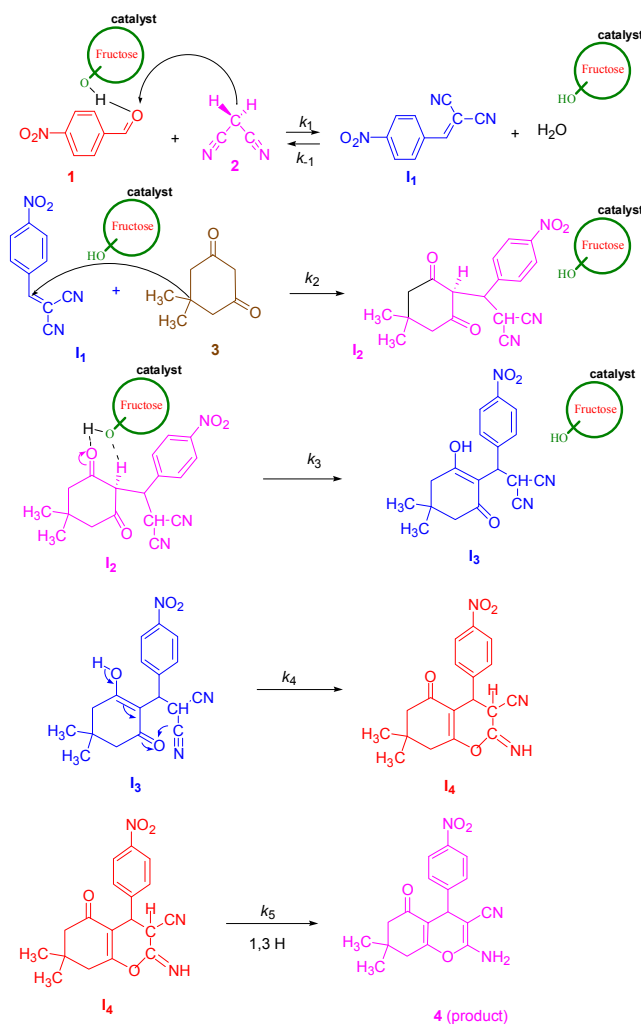


**Fig. 2.** Proposed mechanism of reaction of **1**, **2**, and **3** in the presence of fructose for synthesis of 2-amino-5,6,7,8-tetrahydro-7,7-dimethyl-4-(4-nitrophenyl)-5-oxo-4*H*-chromene-3-carbonitrile (**4**) in H<sub>2</sub>O-EtOH (2:1).

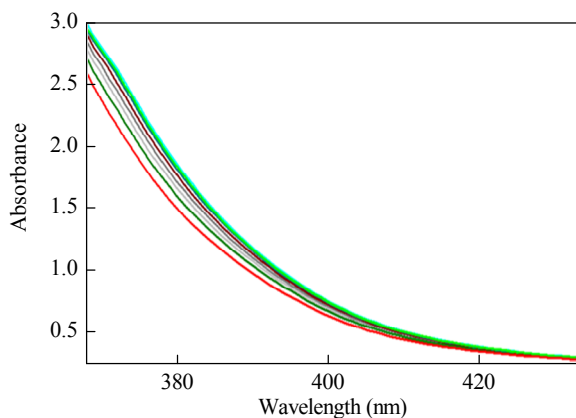


**Fig. 3.** UV-Vis spectra of reaction of 4-nitrobenzaldehyde (**1**; 10 mmol/L), malononitrile (**2**; 10 mmol/L), and dimedone (**3**; 10 mmol/L) in the presence of fructose (25 mmol/L) as a catalyst in H<sub>2</sub>O-EtOH (2:1).

concentrations 10 mmol/L of **1**, **2**, and **3** in the presence of fructose (2.5 mmol/L) in H<sub>2</sub>O-EtOH (2:1) at 25 °C (Fig. 4).

The infinity absorbance ( $A_{\infty}$ ) was obtained at 50 min, as shown in Fig. 4. A second-order fit curve (solid line) was obtained from the absorbance data versus time at 385 nm, which precisely described the experimental curve (dotted line), as shown in Fig. 4 [41]. It is clear that the reaction is second order, therefore the overall order of the rate law can be written as  $\alpha + \beta + \gamma = 2$ , and the original rate law can be written as

$$\text{rate} = k_{\text{ovr}}[\mathbf{1}]^{\alpha}[\mathbf{2}]^{\beta}[\mathbf{3}]^{\gamma}[\text{Cat}] \quad (1)$$

### 3.3. Mechanism

The partial order of reactant **3** under pseudo-order conditions was determined in a separate (fourth) experiment, using the same procedure and the following concentrations: reactant **1** (10 mmol/L); reactant **2** (10 mmol/L); reactant **3** (1 mmol/L); and fructose (2.5 mmol/L). To obtain Eq. (2), the rate law can be expressed as

$$\begin{aligned} \text{rate} &= k_{\text{ovr}}[\mathbf{1}]^{\alpha}[\mathbf{2}]^{\beta}[\mathbf{3}]^{\gamma}[\text{Cat}] \\ \text{rate} &= k_{\text{obs}}[\mathbf{3}]^{\gamma} \\ \text{rate} &= k_{\text{ovr}}[\mathbf{1}]^{\alpha}[\mathbf{2}]^{\beta}[\text{Cat}] \end{aligned} \quad (2)$$

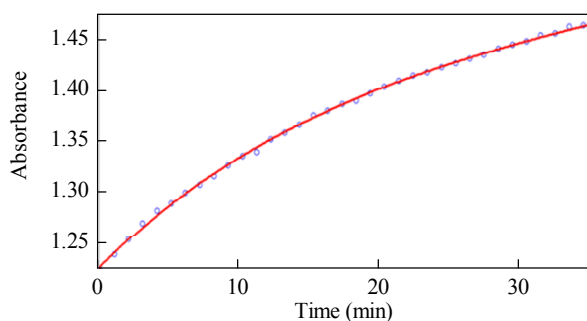


**Fig. 4.** Experimental absorbance changes (dotted line) and fit curve (solid line) against time for reaction of 4-nitrobenzaldehyde (**1**; 0.1 mmol/L), malononitrile (**2**; 0.1 mmol/L), and dimedone (**3**; 0.1 mmol/L) in presence of fructose (25 mmol/L) in H<sub>2</sub>O-EtOH (2:1) at 385 nm and 25.0 °C.

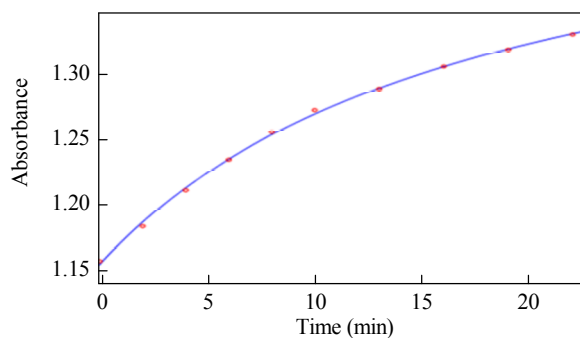


**Fig. 5.** Pseudo-second-order fit curve (solid line) and original experimental curve (dotted) for reaction of dimedone, malononitrile, and 4-nitrobenzaldehyde in the presence of fructose at 385 nm and 25.0 °C in H<sub>2</sub>O-EtOH (2:1).

Here, the original experimental absorbance shows second-order behavior as a function of time. This is shown by the full line at 385 nm, which exactly fits the experimental results (Fig. 5). The rate constant ( $k_{\text{obs}}$ ) was obtained from the experimental curve.

The experimental data show that the observed pseudo-second-order rate constant ( $k_{\text{obs}}$ ) is identical to the second-order rate constant, which implies that  $\gamma = 0$  in Eq. (2).

The results show that the reaction is zero- and second-order with respect to **3** ( $\gamma = 0$ ) and the sum of **1** and **2** ( $\alpha + \beta = 2$ ), respectively.

In a fifth experiment, to determine the partial order of the reaction with respect to 4-nitrobenzaldehyde (**1**), pseudo-order conditions were defined for the reaction of **2** (10 mmol/L), **3** (10 mmol/L), and **1** (10 mmol/L) in the presence of fructose (2.5 mmol/L) in H<sub>2</sub>O-EtOH (2:1). The results show that the rate law can be expressed as

$$\begin{aligned} \text{rate} &= k_{\text{ovr}}[\mathbf{1}]^{\alpha}[\mathbf{2}]^{\beta}[\mathbf{3}]^{\gamma}[\text{Cat}] \\ \text{rate} &= k_{\text{obs}}[\mathbf{1}]^{\alpha} \\ \text{rate} &= k_{\text{ovr}}[\mathbf{2}]^{\beta}[\mathbf{3}]^{\gamma}[\text{Cat}] \end{aligned} \quad (3)$$

The original experimental absorbance versus time (full line) at 385 nm, which exactly fits the experimental curve (dotted line), is shown in Fig. 6.

Fig. 6 shows that it is reasonable to accept that the partial order with respect to reactant **1** is one ( $\alpha = 1$ ). The results of the third ( $\alpha + \beta + \gamma = 2$ ) and fourth ( $\gamma = 0$ ) experiments show that the partial order  $\beta$  is one. The experimental rate law can therefore be expressed as

$$\begin{aligned} \text{rate} &= k_{\text{obs}}[\mathbf{1}][\mathbf{2}] \\ k_{\text{obs}} &= k_1[\text{Cat}] \end{aligned} \quad (4)$$

These results were used to produce a simplified scheme for the proposed reaction mechanism (Fig. 2), and is shown in Fig. 7.

To determine which step in the proposed mechanism is the rate-determining step, the rate law was written using the final reaction step:

$$\text{rate} = k_5[\mathbf{I}_4] \quad (5)$$

The steady-state approximation can be used for  $[\mathbf{I}_1]$ , yielding

$$\frac{d[\mathbf{I}_4]}{dt} = k_4[\mathbf{I}_3][\text{Cat}] - k_5[\mathbf{I}_4] = 0 \quad (6)$$

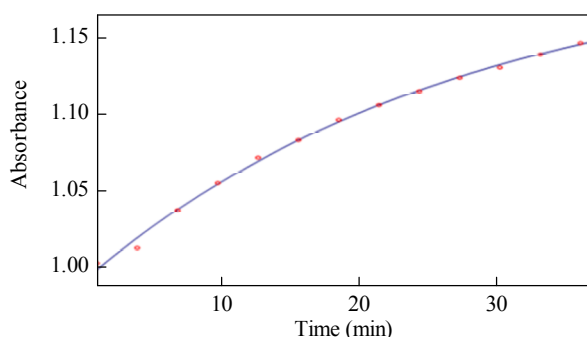


**Fig. 6.** Pseudo-first-order fit curve (solid line) and original experimental curve (dotted line) for reaction of **1**, **2**, and **3** in the presence of fructose at 385 nm and 25.0 °C in H<sub>2</sub>O-EtOH (2:1).

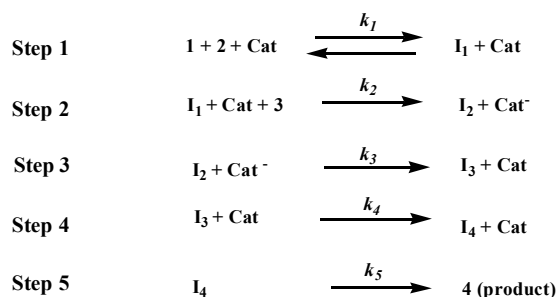


**Fig. 7.** Simplified scheme for proposed reaction mechanism.

$$k_4[\mathbf{I}_3][\text{Cat}] = k_5[\mathbf{I}_4] \quad (7)$$

The value of  $[\mathbf{I}_4]$  can be replaced in Equation (5) to give

$$\text{rate} = k_4[\mathbf{I}_3][\text{Cat}] \quad (8)$$

The  $[\mathbf{I}_3]$  can be determined from the following equation, by applying the steady-state approximation:

$$\frac{d[\mathbf{I}_3]}{dt} = k_3[\mathbf{I}_2][\text{Cat}] - k_4[\mathbf{I}_3][\text{Cat}] = 0 \quad (9)$$

$$k_3[\mathbf{I}_2][\text{Cat}] = k_4[\mathbf{I}_3][\text{Cat}]$$

By substituting Equation (9) into (8) and using some simple mathematics, the following equation is obtained:

$$\text{rate} = k_3[\mathbf{I}_2][\text{Cat}] \quad (10)$$

The steady-state approximation can then be used to determine  $[\mathbf{I}_2]$ , as follows:

$$\frac{d[\mathbf{I}_2]}{dt} = k_2[\mathbf{I}_1][\text{Cat}][\mathbf{1}] - k_4[\mathbf{I}_3][\text{Cat}] = 0 \quad (11)$$

$$k_2[\mathbf{I}_1][\text{Cat}][\mathbf{1}] = k_4[\mathbf{I}_3][\text{Cat}] \quad (12)$$

$$\text{rate} = k_2[\mathbf{I}_1][\text{Cat}][\mathbf{1}] \quad (13)$$

$$\frac{d[\mathbf{I}_1]}{dt} = k_2[\mathbf{1}][\mathbf{2}][\text{Cat}] - k_{-1}[\mathbf{I}_1][\text{Cat}] - k_2[\mathbf{3}][\mathbf{I}_1][\text{Cat}] = 0 \quad (14)$$

$$[\mathbf{I}_1] = \frac{k_2[\mathbf{1}][\mathbf{2}]}{k_{-1} + k_2[\mathbf{3}]} \quad (15)$$

$$\text{rate} = \frac{k_2[\mathbf{3}][\text{Cat}] \times k_1[\mathbf{1}][\mathbf{2}]}{k_{-1} + k_2[\mathbf{3}]} \quad (16)$$

$k_4$ ,  $k_5$  and  $k_3$  are not involved in Eq. (16), therefore these rate constants cannot be those for the rate-determining step, but if  $k_2 \gg k_{-1}$ , the following equations are obtained:

$$\text{rate} = k_1[\mathbf{1}][\mathbf{2}][\text{Cat}] \text{ and } k_{\text{ovc}} = k_1[\text{Cat}] \quad (17)$$

$$\text{rate} = k_{\text{ovc}}[\mathbf{1}][\mathbf{2}] \quad (18)$$

Eq. (18) indicates that the original order of the reaction is two. Additionally, the orders of the reaction with respect to **1**, **2**, and **3** are one, one, and zero, respectively. Also, because of the presence of  $k_1$  in Eq. (18), it is clear that the first step ( $k_1$ ) is the rate-determining step.

### 3.4. Effects of solvents and temperature

To assess the effects of changes in temperature and the solvent environment on the reaction rate, experiments were performed at various temperatures and in solvents with various polarities, with the other conditions the same as those in the earlier experiments.

Because the transition state (Step 1, Fig. 2) in the reaction carries a dispersed charge, solvents with high dielectric constants increase the reaction rate by stabilizing the transition-state species more than the reactants, lowering  $E_a$  (Table 4).

In the temperature range investigated, the relationship between the second-order rate constant ( $\ln k_2$ ) of the reaction with reciprocal temperature conforms to the Arrhenius equation. This is shown in Fig. 8. The activation energy for the reaction of **1**, **2**, and **3** (65.34 kJ/mol) was obtained from the slope of the plot in Fig. 8.

The Eyring equation was used to determine the activation parameters  $\Delta H^\ddagger$  (activation enthalpy),  $\Delta S^\ddagger$  (activation entropy), and  $\Delta G^\ddagger$  (activation Gibbs energy) from the intercept and slope (Fig. 9). According to Equation (18),  $k_1$  is proportional to the general reaction rate, therefore the activation parameters, i.e.,

**Table 4**

Rate constants for reaction of 4-nitrobenzaldehyde (**1**; 10 mmol/L), malononitrile (**2**; 10 mmol/L), and dimedone (**3**; 10 mmol/L) in presence of fructose (2.5 mmol/L) in various solvents and at various temperatures.

Solvent	$\epsilon$	$k_1 \times 10^2$ (L mol <sup>-1</sup> min <sup>-1</sup> )			
		$T = 15^\circ\text{C}$	$T = 20^\circ\text{C}$	$T = 25^\circ\text{C}$	$T = 30^\circ\text{C}$
H <sub>2</sub> O-EtOH (2:1)	60.9	2.97	4.73	6.92	11.75
Methanol	32.6	—	—	—	14.82
Ethanol	24.3	—	—	—	8.25

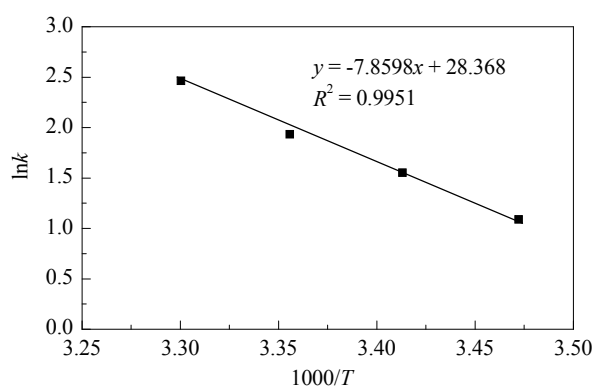


**Fig. 8.** Dependence of second-order rate constant ( $\ln k_1$ ) on reciprocal temperature for reaction of **1**, **2**, and **3** in the presence of fructose, measured at a wavelength of 385 nm, in H<sub>2</sub>O-EtOH (2:1), based on the Arrhenius equation.

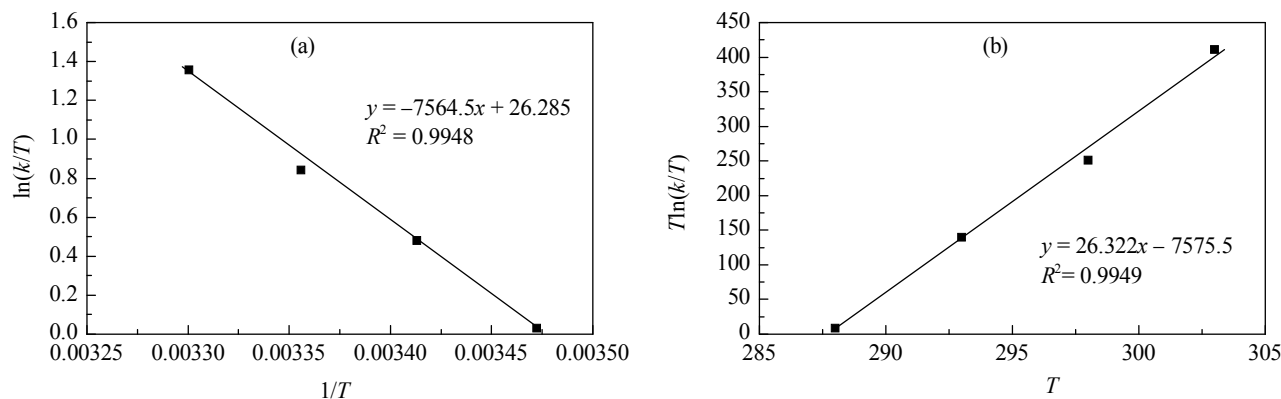


Fig. 9. Eyring plots for reaction of **1**, **2**, and **3** in the presence of fructose in H<sub>2</sub>O-EtOH (2:1).

$\Delta G^\ddagger = 69.14$  kJ/mol,  $\Delta S^\ddagger = 20.99$  J/(mol·K), and  $\Delta H^\ddagger = 62.89$  kJ/mol, can be calculated for the first step (rate-determining step,  $k_1$ ), which is an elementary reaction, based on the Eyring equation.

#### 4. Conclusions

The overall order of the reaction for the formation of a 4*H*-tetrahydrobenzo[*b*]pyran derivative in the presence of fructose followed second-order kinetics, and the partial orders with respect to 4-nitrobenzaldehyde (**1**), malononitrile (**2**), and dimedone (**3**) were one, one, and zero, respectively. The results show that rate of reaction increases in solvents with high dielectric constants at all temperatures. In the studied temperature range, the second-order rate constant of the reaction was inversely proportional to the temperature, in agreement with the Arrhenius equation. The first step of the proposed mechanism was identified as the rate-determining step ( $k_1$ ), and this was confirmed based on the steady-state approximation.

The yield was a function of temperature, because the yield increased with increasing temperature; at 40 °C, the product was obtained in excellent yield, but the yield did not increase at higher temperatures. Moreover, 20 mol% was chosen as a suitable amount of catalyst for this reaction.

#### References

- [1] Alvey L, Prado S, Huteau V, Saint-Joanis B, Michel S, Koch M, Cole S T, Tillequin F, Janin Y L. *Bioorg Med Chem*, 2008, 16: 8264
- [2] Symeonidis T, Chamilos M, Hadjipavlou-Litina D J, Kallitsakis M, Litinas K E. *Bioorg Med Chem Lett*, 2009, 19: 1139
- [3] Narender T, Shweta, Gupta S. *Bioorg Med Chem Lett*, 2004, 14: 3913
- [4] Lakshmi V, Pandey K, Kapil A, Singh N, Samant M, Dube A. *Phyto-medicine*, 2007, 14: 36
- [5] Kumar D, Reddy V B, Sharad S, Dube U, Kapur S. *Eur J Med Chem*, 2009, 44: 3805
- [6] El-Agrody A M, El-Hakim M H, El-Latif M S A, Fakery A H, El-Sayed E S M, El-Ghareab K A. *Acta Pharm*, 2000, 50: 111
- [7] Konkoy C S, Fick D B, Cai S X, Lan N C, Keana J F W. *Chem Abstr*, 2001, 134a: 29313
- [8] Niknam K, Borazjani N, Rashidian R, Jamali A. *Chin J Catal*, 2013, 34: 2245
- [9] Devi I, Bhuyan P J. *Tetrahedron Lett*, 2004, 45: 8625
- [10] Tu S J, Jiang H, Zhong Q Y, Miu C B, Shi D Q, Wang X S, Gao Y. *Chin J Org Chem*, 2003, 23: 488
- [11] Jin T S, Wang A Q, Shi F, Han L S, Liu L B, Li T S. *Arkivoc*, 2006: 78
- [12] Balalaie S, Shiekh-Ahmadi M, Bararjanian M. *Catal Commun*, 2007, 8: 1724
- [13] Abdolmohammadi S, Balalaie S. *Tetrahedron Lett*, 2007, 48: 3299
- [14] Gao S, Tsai C H, Tseng C, Yao C F. *Tetrahedron*, 2008, 64: 9143
- [15] Seifi M, Sheibani H. *Catal Lett*, 2008, 126: 275
- [16] Hekmatshoar R, Majedi S, Bakhtiari K. *Catal Commun*, 2008, 9: 307
- [17] Ren Y M, Cai C. *Catal Commun*, 2008, 9: 1017
- [18] Heravi M M, Jani B A, Derikvand F, Bamoharram F F, Oskooie H A. *Catal Commun*, 2008, 10: 272
- [19] Khurana J M, Kumar S. *Tetrahedron Lett*, 2009, 50: 4125

#### Graphical Abstract

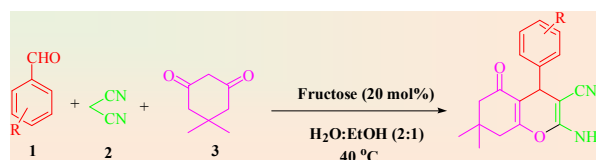
*Chin. J. Catal.*, 2015, 36: 757–763 doi: 10.1016/S1872-2067(14)60302-8

#### Fructose-catalyzed synthesis of tetrahydrobenzo[*b*]pyran derivatives: Investigation of kinetics and mechanism

Sayyedah Shadfar Pourpanah, Sayyed Mostafa Habibi-Khorassani\*, Mehdi Shahraki

University of Sistan and Baluchestan, Iran

We report kinetic results and detailed mechanistic studies for the synthesis of a derivative of 4*H*-tetrahydrobenzo[*b*]pyran, based on a global kinetic analysis method using UV-Vis spectroscopy.



- [20] Sabitha G, Arundhathi K, Sudhakar K, Sastry B S, Yadav J S. *Synth Commun*, 2009, 39: 433
- [21] Sun W B, Zhang P, Fan J, Chen S H, Zhang Z H. *Synth Commun*, 2010, 40: 587
- [22] Wang L M, Shao J H, Tian H, Wang Y H, Liu B. *J Fluorine Chem*, 2006, 127: 97
- [23] Khodaei M M, Bahrami K, Farrokhi A. *Synth Commun*, 2010, 40: 1492
- [24] Fang D, Zhang H B, Liu Z L. *J Heterocycl Chem*, 2010, 47: 63
- [25] Li Y C, Chen H, Shi C L, Shi D Q, Ji S J. *J Comb Chem*, 2010, 12: 231
- [26] Katkar S S, Lande M K, Arbad B R, Gaikwad S T. *Chin J Chem*, 2011, 29: 199
- [27] Zheng J, Li Y Q. *Scholar Research Library*, 2011, 3: 381
- [28] Salvi P P, Mandhare A M, Sartape A S, Pawar D K, Han S H, Kolekar S S. *C R Chim*, 2011, 14: 878
- [29] Karami B, Kiani M, Ahmad Hoseini M. *Chin J Catal*, 2014, 35: 1206
- [30] Wei J W, Guo W G, Zhang B Y, Liu Y, Li C. *Chin J Catal*, 2014, 35: 1008
- [31] Hazeri N, Maghsoodlou M T, Mir F, Kangani M, Saravani H, Mollashahi E. *Chin J Catal*, 2014, 35: 391
- [32] Kangani M, Hazeri N, Maghsoodlou M, Salahi S. *Res Chem Intermed*, 2013, doi: 10.107/s11164-013-1365-z
- [33] Mousavi M R, Hazeri N, Maghsoodlou M T, Salahi S, Habibi-Khorassani S M. *Chin Chem Lett*, 2013, 24: 411
- [34] Noorisadeh F, Maghsoodlou M T, Hazeri N, Kangani M. *Res Chem Intermed*, 2014, doi:10.1007/s11164-014-1710-x
- [35] Habibi-Khorassani S M, Ebrahimi A, Maghsoodlou M T, Asheri O, Shahraki M, Akbarzadeh N, Ghalandarzehi Y. *Int J Chem Kinet*, 2013, 45: 596
- [36] Habibi-Khorassani S M, Maghsoodlou M T, Ebrahimi A, Farahani F V, Mosaddeg E, Kazemian M A. *Tetrahedron Letters*, 2009, 50: 3621
- [37] Habibi-Khorassani S M, Ebrahimi A, Maghsoodlou M T, Zakari-anezhad M, Ghasempour H, Ghahghayi Z. *Curr Org Chem*, 2011, 15: 942
- [38] Dehdab M, Habibi-Khorassani S M, Shahraki M. *Catal Lett*, 2014, 144: 1790
- [39] Jin T S, Wang A Q, Wang X, Zhang J S, Li T S. *Synlett*, 2004: 871
- [40] Gurumurthi S, Sundari V, Valliappan R. *E-J Chem*, 2009, 6: S466
- [41] Schwartz L M, Gelb R I. *Anal Chem*, 1978, 50: 1592